Development and analysis of a two-stage beamformer for multiple correlated interferers using rectangular array

T.-T. Lin and T.-S. Lee[a)]
Department of Communication Engineering, National Chiao Tung University, Hsinchu, Taiwan, Republic of China

(Received 8 July 1995; revised 24 July 1998; accepted 7 October 1998)

A two-stage two-dimensional (2-D) beamformer is proposed for signal enhancement in an environment of multiple correlated interferers using a rectangular array. In the first stage, subarray beamformers are constructed which exhibit reliable interference cancellation using difference-preprocessed and spatially smoothed data. A secondary combining of all possible subarray beamformers is then performed to fully exploit the array aperture. It is shown that, compared to the conventional one-stage optimum beamformer, the two-stage beamformer performs equally well and requires a much lower complexity of implementation when a suitable subarray size is chosen. [S0001-4966(99)04701-3]

PACS numbers: 43.60.Dh, 43.60.Gk [JCB]

INTRODUCTION

An adaptive beamformer performs spatial filtering by forming a beam in such a fashion that the desired signal can be received with a large gain, while unwanted interference and noise can be suppressed.[1] It has a wide range of acoustical applications, including sound-signal enhancement and underwater communications.[2–4] Conventional adaptive beamformers are effective in suppressing strong interference so long as the pointing error is small and the interferers are uncorrelated with the desired source. However, in the presence of beam-pointing errors and/or highly correlated interferers, these beamformers exhibit severe degradation in the output signal-to-interference-plus-noise ratio (SINR) as a result of signal cancellation.[5,6] To avoid such problems, the difference preprocessor[5] was proposed as a tool for removing the desired signal before beamforming. By difference preprocessing, the beamformer will not cancel the desired signal even in the presence of pointing errors and coherent interference.

In spite of the success of dealing with a single correlated interferer, the difference-preprocessed beamformer cannot handle multiple correlated interferers.[7] This is because the relationship that causes the mutual cancellation between the multiple interfering signals in the master beamformer is destroyed as the optimum weights are copied to the slave beamformer. To avoid such performance breakdown, the spatial-smoothing technique[8] was incorporated as a means of decorrelating the interfering signals. This ensures that the beamformer will suppress each of the interfering signals, instead of performing a mutual cancellation. Unfortunately, working with spatial smoothing results in a reduction of the array aperture, which in turn reduces the signal-to-noise ratio (SNR) gain, nulling capacity and resolution capability of the beamformer. A post combiner can be employed to recover the full aperture of the array.[7,9] This means that the weight vector associated with the (spatially smoothed) subarray beamformer is copied to each of the possible subarrays of the same size, and the overall beamformer is obtained via a secondary combining of all subarray beamformers.

We exploit here the post-combining concept to develop a two-stage 2-D beamformer for rectangular arrays. The beamformer first incorporates a 2-D difference preprocessor to alleviate desired signal cancellation due to pointing errors. The 2-D spatial smoothing[10] is then employed to decorrelate the interference left in the preprocessor output, leading to a rectangular subarray. The spatially smoothed correlation matrix is noise whitened and used to compute the 2-D weights which produce a null in each of the interfering directions. This set of weights can be applied back to each of the identical subarrays, leading to a set of ''interference cancellation'' beamformers. Finally, a full-aperture beamformer is obtained via a secondary combining of the interference-free subarray beamformers in accordance with the maximum-output SNR criterion. The two-stage procedure is algebraically organized in that each type of 2-D operation involved is represented by a matrix transformation, which facilitates the derivation of the correlation structure and weight vector. The proposed 2-D beamformer is suitable for acoustical signal acquisition in the presence of multipath reflections and strong interference. For example, the beamformer can be implemented on a microphone array[2] for remote sound-source analysis in an indoor environment contaminated with narrow-band manmade noise. It can also be used for acoustical communications in shallow water, where multipaths cause a major problem.[4] On the other hand, the algorithm for computing the 2-D weights can be executed in an adaptive fashion by using high-speed digital signal processors.[3,4] In this regard, the two-stage procedure is much more efficient than the conventional one-stage procedure in that the computational complexity is significantly reduced by breaking the original large 2-D array into two smaller ones.

[a)]Electronic mail: tslee@cc.nctu.edu.tw

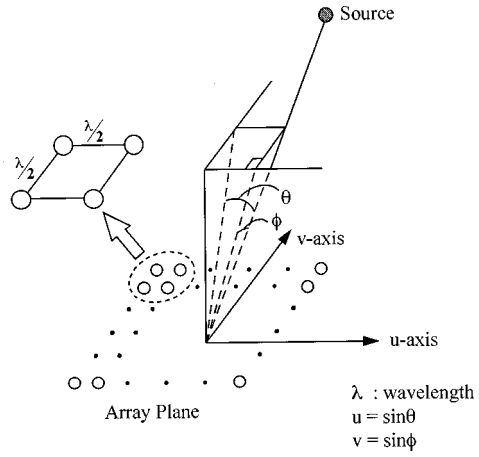

FIG. 1. Array geometry and coordinate system.

I. PROBLEM FORMULATION

A. Notations

Some of the key notations are defined as follows:

$\cdot^T(\cdot^H)$:	transpose (complex conjugate transpose)
$\mathbf{I}_n$:	$n\times n$ identity matrix
$\mathbf{J}_n$:	$n\times n$ reverse permutation matrix with ones on the antidiagonal and zeros elsewhere
$\mathbf{O}_{m\times n}$:	$m\times n$ zero matrix
$\mathbf{M}(i,k)$:	(i,k)th entry of matrix $\mathbf{M}$
$\mathbf{M}(i:k,l:m)$:	submatrix of entries from ith to kth rows and lth to mth columns of $\mathbf{M}$
Vec$\{\mathbf{M}\}$:	concatenation of columns of $m\times n$ matrix $\mathbf{M}$ into $mn\times 1$ column vector
Vec$^{-1}\{\mathbf{v}\}$:	inverse of $\mathbf{v}=$Vec$\{\mathbf{M}\}$
$\mathbf{L}\odot\mathbf{M}$:	Inner product of matrices $\mathbf{L}$ and $\mathbf{M}$ defined by $\mathbf{L}\odot\mathbf{M}=\sum_i\sum_k \mathbf{L}^*(i,k)\mathbf{M}(i,k)$ $=\text{Vec}^H\{\mathbf{L}\}\text{Vec}\{\mathbf{M}\}$.
Diag$\{\mathbf{v}\}$:	diagonal matrix whose main diagonal entries are given by vector $\mathbf{v}$
$E\{\cdot\}$:	expectation
Corr$\{\mathbf{v}\}$:	correlation matrix of random vector $\mathbf{v}$ defined by Corr$\{\mathbf{v}\}=E\{\mathbf{v}\mathbf{v}^H\}$.

B. Array-data model

Consider the scenario involving a desired source and K possibly correlated interferers impinging on an $M\times N$ narrow-band rectangular array of identical elements equally spaced by a half-wavelength. These sources are assumed to be in the far field of the array such that the plane-wave model holds. The array data received at a certain sampling instant can be expressed as an $M\times N$ matrix:

$$\mathbf{X}=\sum_{i=1}^{K+1}\xi_i\mathbf{A}(u_i,v_i)+\mathbf{N}, \tag{1}$$

where $u_i=\sin(\theta_i)$ and $v_i=\sin(\phi_i)$ represent the sine-space angles of the ith source with respect to the u- and v-axis, respectively, as shown in Fig. 1. Note that the coordinate system inherently imposes the constraint $|\theta|+|\phi|\leqslant 90$ deg. The random scalar ξ_i denotes the complex envelop of the ith source received at the (1,1)th element of the array, and $\sigma_i^2=E\{|\xi_i|^2\}$ is the corresponding source power. The $M\times N$ matrix $\mathbf{A}(u,v)$ is the array-response matrix given by

$$\mathbf{A}(u,v)=\mathbf{a}_M(u)\mathbf{a}_N^T(v), \tag{2}$$

where

$$\begin{aligned}\mathbf{a}_m(u)&=[1,e^{j\pi u},\ldots,e^{j(m-1)\pi u}]^T\\ \mathbf{a}_n(v)&=[1,e^{j\pi v},\ldots,e^{j(n-1)\pi v}]^T\end{aligned} \tag{3}$$

[with $m=M$ and $n=N$ in (2)] are the 1-D response vectors along the u- and v-axis, respectively. Finally, $\mathbf{N}$ consists of the noise present at the elements. In the following development, we will assume that source 1 is the desired one and treat the others as interference. Also, the noise components in $\mathbf{N}$ are assumed spatially white with power σ_n^2.

One way of viewing the data matrix in $MN\times 1$ vector form is by concatenating the columns (u axis) of $\mathbf{X}$ into

$$\mathbf{x}=\text{Vec}\{\mathbf{X}\}=\sum_{i=1}^{K+1}\xi_i\mathbf{a}(u_i,v_i)+n=\mathbf{D}\mathbf{s}+\mathbf{n}, \tag{4}$$

where

$$\mathbf{a}(u,v)=\text{Vec}\{\mathbf{A}(u,v)\} \tag{5}$$

$$\mathbf{D}=[\mathbf{a}(u_1,v_1),\mathbf{a}(u_2,v_2),\ldots,\mathbf{a}(u_{K+1},v_{K+1})] \tag{6}$$

$$\mathbf{s}=[\xi_1,\xi_2,\ldots,\xi_{K+1}]^T \tag{7}$$

$$\mathbf{n}=\text{Vec}\{\mathbf{N}\}. \tag{8}$$

We refer to $\mathbf{x}$, $\mathbf{a}(u,v)$, and $\mathbf{n}$ as the vector representations of $\mathbf{X}$, $\mathbf{A}(u,v)$, and $\mathbf{N}$, respectively.

C. Beamforming issues

A beamformer transforms the array-data matrix into a scalar output y via an $M\times N$ weight matrix $\mathbf{W}$ according to

$$y=\mathbf{W}\odot\mathbf{X}=\mathbf{w}^H\mathbf{x}, \tag{9}$$

where $\mathbf{w}=\text{Vec}\{\mathbf{W}\}$ is the vector representation of $\mathbf{W}$ corresponding to $\mathbf{x}$.

The beamformer we will work with is the linearly constrained minimum variance (LCMV) beamformer,[11] which minimizes the output power subject to a fixed-response constraint in the look direction $(u_o,v_o)=[\sin(\theta_o),\sin(\phi_o)]$:

$$\min_{\mathbf{w}} E\{|y|^2\}\equiv\mathbf{w}^H\mathbf{R}_x\mathbf{w}$$
$$\text{subject to: } \mathbf{W}\odot\mathbf{A}(u_o,v_o)\equiv\mathbf{w}^H\mathbf{a}(u_o,v_o)=c, \tag{10}$$

where $\mathbf{R}_x$ is the $MN\times MN$ data-correlation matrix, and c is a nonzero constant. Invoking the spatial whiteness of $\mathbf{N}$ and using (4), we have

$$\mathbf{R}_x=\text{Corr}\{\mathbf{x}\}=\mathbf{D}\mathbf{P}\mathbf{D}^H+\sigma_n^2\mathbf{I}_{MN}, \tag{11}$$

where $\mathbf{P}=\text{Corr}\{\mathbf{s}\}$ and $\sigma_n^2\mathbf{I}_{MN}$ are the source and noise correlation matrices, respectively. The solution to (10) is

$$\mathbf{w}=\frac{\sigma_n^2}{\sqrt{MN}}\mathbf{R}_x^{-1}\mathbf{a}(u_o,v_o), \tag{12}$$

where we choose the scaling factor for the convenience of the subsequent analysis.

II. DIFFERENCE PREPROCESSING

The difference preprocessing technique[5] was proposed as a means of avoiding desired signal cancellation due to pointing errors or coherent interference. Although the technique was developed originally for uniform linear array, it can be equally incorporated into the 2-D array considered herein. Note first that an $M\times N$ rectangular array can be viewed as consisting of four identical rectangular subarrays of size $(M-1)\times(N-1)$. By linearly combining these subarrays with a judiciously chosen weight vector $\mathbf{h}=[h_{11},h_{21},h_{12},h_{22}]^T$, a difference preprocessed (DP) virtual subarray results. The DP subarray is an $(M-1)\times(N-1)$ rectangular array whose elements share the same response pattern:

$$h(u,v)=\mathbf{h}^H\mathbf{a}_q(u,v), \tag{13}$$

where

$$\mathbf{a}_q(u,v)=[1,e^{j\pi u},e^{j\pi v},e^{j\pi(u+v)}]^T \tag{14}$$

accounts for the relative phases among the four subarrays. By difference preprocessing, the desired signal is removed by choosing $\mathbf{h}$ such that $h(u_o,v_o)=0$.

Denote as

$$\tilde{\mathbf{A}}(u,v)=\mathbf{a}_{M-1}(u)\mathbf{a}_{N-1}^T(v) \tag{15}$$

$$\tilde{\mathbf{a}}(u,v)=\mathrm{Vec}\{\tilde{\mathbf{A}}(u,v)\} \tag{16}$$

$$\tilde{\mathbf{D}}=[\tilde{\mathbf{a}}(u_1,v_1),\tilde{\mathbf{a}}(u_2,v_2),\ldots,\tilde{\mathbf{a}}(u_{K+1},v_{K+1})] \tag{17}$$

the counterparts of $\mathbf{A}(u,v)$, $\mathbf{a}(u,v)$, and $\mathbf{D}$, respectively, for the DP subarray. The operation of the preprocessor yields the DP data matrix as given by

$$\tilde{\mathbf{X}}=\sum_{i=1}^{2}\sum_{k=1}^{2}h_{ik}^*\mathbf{X}(i:M+i-2,k:N+k-2). \tag{18}$$

Since the effect of difference preprocessing is to scale the ith signal with the complex gain $h(u_i,v_i)$, we can show that the vector representation of $\tilde{\mathbf{X}}$ is

$$\tilde{\mathbf{x}}=\mathrm{Vec}\{\tilde{\mathbf{X}}\}=\mathbf{H}^H\mathbf{x}=\tilde{\mathbf{D}}\mathbf{G}\mathbf{s}+\mathbf{H}^H\mathbf{n}, \tag{19}$$

where

$$\mathbf{G}=\mathrm{Diag}\{[h(u_1,v_1),h(u_2,v_2),\ldots,h(u_{K+1},v_{K+1})]^T\} \tag{20}$$

accounts for the preprocessor gain for the $K+1$ sources, and

$$\mathbf{H}=\begin{bmatrix}\mathbf{H}_1 & & & 0\\ \mathbf{H}_2 & \mathbf{H}_1 & & \\ & \mathbf{H}_2 & \ddots & \\ & & \ddots & \mathbf{H}_1\\ 0 & & & \mathbf{H}_2\end{bmatrix}_{MN\times(M-1)(N-1)} \tag{21}$$

with

$$\mathbf{H}_i=\begin{bmatrix}h_{1i} & & & 0\\ h_{2i} & h_{1i} & & \\ & h_{2i} & \ddots & \\ & & \ddots & h_{1i}\\ 0 & & & h_{2i}\end{bmatrix}_{M\times(M-1)} \qquad i=1,2 \tag{22}$$

is the matrix representation of the preprocessor operation in (18). Note that the Toeplitz–block–Toeplitz structure of $\mathbf{H}$, as a result of the rectangular-array geometry, leads to $\mathbf{H}^H\mathbf{D}=\tilde{\mathbf{D}}\mathbf{G}$. The expression in (19) makes it easy to derive the DP data-correlation matrix:

$$\tilde{\mathbf{R}}_x=\mathrm{Corr}\{\tilde{\mathbf{x}}\}=\tilde{\mathbf{D}}\mathbf{G}\mathbf{P}\mathbf{G}^*\tilde{\mathbf{D}}^H+\sigma_n^2\mathbf{H}^H\mathbf{H}, \tag{23}$$

which indicates that on the DP subarray, one observes the source-correlation matrix $\mathbf{GPG}^*$ and noise-correlation matrix $\sigma_n^2\mathbf{H}^H\mathbf{H}$.

A. Separable preprocessor

The separable preprocessor is a direct extension of the 1-D preprocessor obtained by choosing $\mathbf{h}=[1,-e^{j\pi u_o},-e^{j\pi v_o},e^{j\pi(u_o+v_o)}]^T$. It is called separable since the response pattern $h(u,v)=[1-e^{j\pi(u-u_o)}][1-e^{j\pi(v-v_o)}]$ is separable with respect to the two axes. Figure 2(a) shows that the preprocessor produces a cross-null pattern centered at $(\theta_o,\phi_o)=(0\text{ deg},0\text{ deg})$. This causes the problem that the preprocessor will eliminate interferes from either (u,v_o) or (u_o,v), where u and v can be arbitrary. If this is the case, then the beamformer attached to the preprocessor cannot ''see'' these interferes and will fail to cancel them.

B. Nonseparable preprocessor

To avoid interference cancellation by the preprocessor, the response pattern $h(u,v)$ should exhibit nulling only within a limited region around (u_o,v_o). A possible approach is as follows. First, the constraint $h(u_o,v_o)=0$ is guaranteed by forcing $\mathbf{h}=\mathbf{V}_q\mathbf{f}$, where $\mathbf{V}_q$ is the 4×3 matrix representation of the nullspace of $\mathbf{a}_q^H(u_o,v_o)$ and $\mathbf{f}$ is a 3×1 vector. Second, in order to enhance the robustness of the preprocessor against pointing errors, the response $h(u,v)$ should be minimized over an angular region R around (u_o,v_o). Third, to retain the interference scenario as much as possible, $h(u,v)$ should be as close to 1 as possible outside R. These requirements lead to the following constrained problem:

$$\begin{aligned}\min_{\mathbf{f}}&\int\int_R|h(u,v)|^2du\,dv+\epsilon\int\int_{\bar{R}}|h(u,v)-1|^2du\,dv\\ &\equiv\mathbf{f}^H\mathbf{V}_q^H\mathbf{T}\mathbf{V}_q\mathbf{f}+\epsilon\left[\mathbf{f}^H\mathbf{V}_q^H\bar{\mathbf{T}}\mathbf{V}_q\mathbf{f}-\mathbf{f}^H\mathbf{V}_q^H\bar{\mathbf{t}}_1-\bar{\mathbf{t}}_1^H\mathbf{V}_q\mathbf{f}\right.\\ &\quad\left.+\int\int_R du\,dv\right]\quad\text{subject to:}\quad\mathbf{f}^H\mathbf{i}_1=1\end{aligned} \tag{24}$$

where

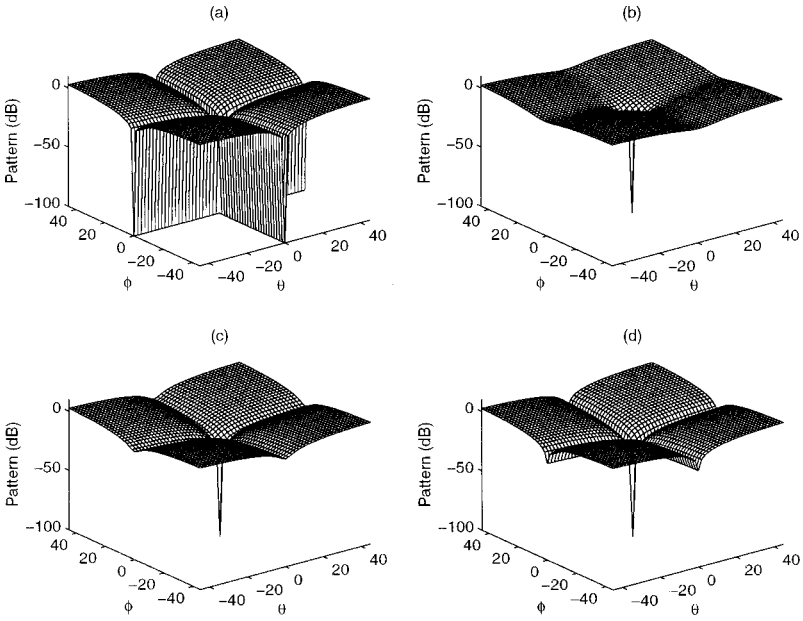

FIG. 2. Patterns of difference preprocessors. (a) separable preprocessor. (b) nonseparable preprocessor with $\epsilon=10^{-2}$. (c) nonseparable preprocessor with $\epsilon=10^{-4}$. (d) nonseparable preprocessor with $\epsilon=10^{-6}$.

$$\mathbf{T}=\int\int_R \mathbf{a}_q(u,v)\mathbf{a}_q^H(u,v)du\ dv \tag{25}$$

$$\overline{\mathbf{T}}=\int\int_{\overline{R}} \mathbf{a}_q(u,v)\mathbf{a}_q^H(u,v)du\ dv. \tag{26}$$

$\overline{\mathbf{t}}_1$ is the first column of $\overline{\mathbf{T}}$, $\mathbf{i}_1=[1,0,0]^T$, and ϵ is a parameter controlling the relative emphasis of the two cost terms. The constraint is included simply to avoid a trivial solution. Using the Lagrange multiplier technique, along with some algebraic manipulation, we get

$$\mathbf{h}=\mathbf{V}_q[\mathbf{V}_q^H(\mathbf{T}+\epsilon\overline{\mathbf{T}})\mathbf{V}_q]^{-1}[\epsilon\mathbf{V}_q^H\mathbf{t}_1+\eta\mathbf{i}_1], \tag{27}$$

where

$$\eta=\frac{1-\epsilon\overline{\mathbf{t}}_1^H\mathbf{V}_q[\mathbf{V}_q^H(\mathbf{T}+\epsilon\overline{\mathbf{T}})\mathbf{V}_q]^{-1}\mathbf{i}_1}{\mathbf{i}_1^H[\mathbf{V}_q^H(\mathbf{T}+\epsilon\overline{\mathbf{T}})\mathbf{V}_q]^{-1}\mathbf{i}_1}. \tag{28}$$

An example of the nonseparable preprocessor is given in Fig. 2(b)–(d), with $R=\{-5\ \text{deg}\leqslant\theta\leqslant 5\ \text{deg}, -5\ \text{deg}\leqslant\phi\leqslant 5\ \text{deg}\}$, $\overline{R}$ being the complement of R, and $\epsilon=10^{-2}$, 10^{-4}, and 10^{-6}, respectively. As expected, the modified preprocessor does not produce the cross-null pattern as in Fig. 2(a). Furthermore, a comparison of these patterns gives an indication as to how a tradeoff between desired signal removal in R and flatness of response in $\overline{R}$ can be achieved with a suitably chosen ϵ.

III. 2-D SPATIAL SMOOTHING

In the presence of multiple correlated interferers, as usually incurred with multipath propagation, the beamformer operating on the DP data cannot cancel these interferes individually. A remedy suitable for the rectangular array is to perform 2-D spatial smoothing[10] on the DP subarray before beamforming. Performing spatial smoothing in this fashion requires that the DP subarray be decomposed into $L=(M-M_1)(N-N_1)$ contiguous overlapping subarrays of size $M_1\times N_1$, as shown in Fig. 3, and that a spatially smoothed (SS) correlation matrix $\overline{\mathbf{R}}_x$ be formed as an average of the correlation matrices associated with these subarrays. With this operation, $\overline{\mathbf{R}}_x$ can be regarded as the correlation matrix associated with an $M_1\times N_1$ virtual subarray on which the desired signal has been removed and the interferes have been decorrelated. We refer to this subarray as the SS subarray, and denote as

$$\overline{\mathbf{A}}(u,v)=\mathbf{a}_{M_1}(u)\mathbf{a}_{N_1}^T(v) \tag{29}$$

$$\overline{\mathbf{a}}(u,v)=\text{Vec}\{\overline{\mathbf{A}}(u,v)\} \tag{30}$$

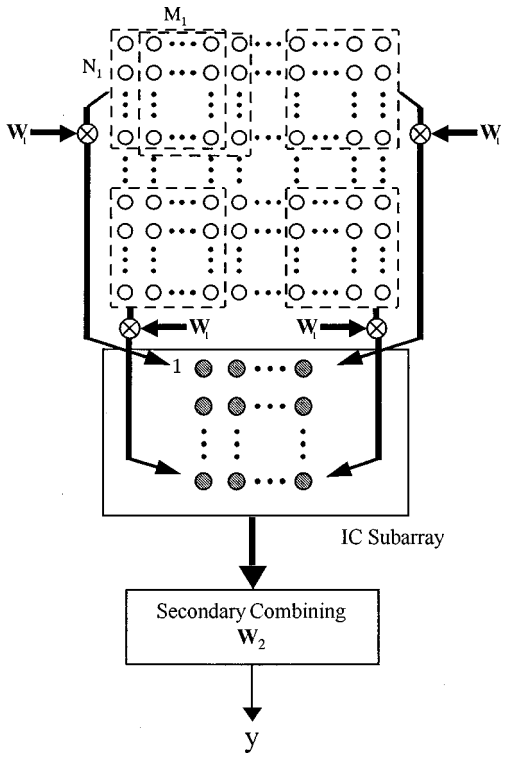

FIG. 3. Subarray configuration and schematic description of two-stage beamforming.

$$\overline{\mathbf{D}}=[\overline{\mathbf{a}}(u_1,v_1),\overline{\mathbf{a}}(u_2,v_2),\ldots,\overline{\mathbf{a}}(u_{K+1},v_{K+1})] \tag{31}$$

the counterparts of $\mathbf{A}(u,v)$, $\mathbf{a}(u,v)$, and $\mathbf{D}$, respectively, associated with it.

The symmetry of rectangular-array geometry allows for the incorporation of the forward–backward (FB) technique[12] to enhance the decorrelation effect of spatial smoothing. That is, we use the fact that

$$\mathbf{J}_{M_1N_1}\overline{\mathbf{a}}^*(u,v)=e^{-j\pi((M_1-1)u+(N_1-1)v)}\overline{\mathbf{a}}(u,v) \tag{32}$$

to double the effective number of subarrays. The FB–SS data-correlation matrix is thus formed by

$$\begin{aligned}\overline{\mathbf{R}}_x=&\frac{1}{2L}\sum_{i=1}^{M-M_1}\sum_{k=1}^{N-N_1}(\mathrm{Corr}\{\mathrm{Vec}\{\tilde{\mathbf{X}}(i:i+M_1-1,\\&k:k+N_1-1)\}\}\\&+\mathrm{Corr}\{\mathbf{J}_{M_1N_1}\mathrm{Vec}\{\tilde{\mathbf{X}}^*(i:i+M_1-1,k:k+N_1-1)\}\})\\=&\frac{1}{2L}\sum_{i=1}^{M-M_1}\sum_{k=1}^{N-N_1}(\mathbf{E}_{ik}\tilde{\mathbf{R}}_x\mathbf{E}_{ik}^T+\mathbf{J}_{M_1N_1}\mathbf{E}_{ik}\tilde{\mathbf{R}}_x^*\mathbf{E}_{ik}^T\mathbf{J}_{M_1N_1})\\=&\overline{\mathbf{R}}_s+\sigma_n^2\overline{\mathbf{R}}_n,\end{aligned} \tag{33}$$

where

$$\mathbf{E}_{ik}=\left[\begin{array}{c|ccc|c}\mathbf{O}_{M_1N_1\times(M-1)(k-1)} & \mathbf{F}_i & & 0 & \mathbf{O}_{M_1N_1\times(M-1)(N-N_1-k)}\\ & & \mathbf{F}_i & & \\ & 0 & & \ddots & \\ & & & \mathbf{F}_i & \end{array}\right] \tag{34}$$

with

$$\mathbf{F}_i=[\mathbf{O}_{M_1\times(i-1)}|\mathbf{I}_{M_1}|\mathbf{O}_{M_1\times(M-M_1-i)}] \tag{35}$$

is the selection matrix picking up the correlation matrix associated with the (i,k)th block $\tilde{\mathbf{X}}(i:i+M_1-1,k:k+N_1-1)$ from $\tilde{\mathbf{R}}_x$. The effective SS signal-only and noise-correlation matrices are given accordingly by

$$\begin{aligned}\overline{\mathbf{R}}_s=&\frac{1}{2L}\sum_{i=1}^{M-M_1}\sum_{k=1}^{N-N_1}(\mathbf{E}_{ik}\tilde{\mathbf{D}}\mathbf{G}\mathbf{P}\mathbf{G}^*\tilde{\mathbf{D}}^H\mathbf{E}_{ik}^T\\&+\mathbf{J}_{M_1N_1}\mathbf{E}_{ik}\tilde{\mathbf{D}}^*\mathbf{G}^*\mathbf{P}^*\mathbf{G}\tilde{\mathbf{D}}^T\mathbf{E}_{ik}^T\mathbf{J}_{M_1N_1})\\=&\overline{\mathbf{D}}\left[\frac{1}{2L}\sum_{i=1}^{M-M_1}\sum_{k=1}^{N-N_1}(\mathbf{\Phi}_{ik}\mathbf{G}\mathbf{P}\mathbf{G}^*\mathbf{\Phi}_{ik}^*\right.\\&\left.+\mathbf{\Psi}\mathbf{\Phi}_{ik}^*\mathbf{G}^*\mathbf{P}^*\mathbf{G}\mathbf{\Phi}_{ik}\mathbf{\Psi}^*)\right]\overline{\mathbf{D}}^H\end{aligned} \tag{36}$$

$$\begin{aligned}\overline{\mathbf{R}}_n=&\frac{1}{2L}\sum_{i=1}^{M-M_1}\sum_{k=1}^{N-N_1}(\mathbf{E}_{ik}\mathbf{H}^H\mathbf{H}\mathbf{E}_{ik}^T\\&+\mathbf{J}_{M_1N_1}\mathbf{E}_{ik}\mathbf{H}^T\mathbf{H}^*\mathbf{E}_{ik}^T\mathbf{J}_{M_1N_1}),\end{aligned} \tag{37}$$

where

$$\mathbf{\Phi}_{ik}=\mathrm{Diag}\left\{\begin{bmatrix}e^{j\pi((i-1)u_1+(k-1)v_1)}\\e^{j\pi((i-1)u_2+(k-1)v_2)}\\\vdots\\e^{j\pi((i-1)u_{K+1}+(k-1)v_{K+1})}\end{bmatrix}\right\}$$

$$i=1,\ldots,M-M_1,\quad k=1,\ldots,N-N_1 \tag{38}$$

accounts for the relative phase shifts among the data blocks $\tilde{X}(i:i+M_1-1,k:k+N_1-1)$, and

$$\mathbf{\Psi}=\mathrm{Diag}\left\{\begin{bmatrix}e^{-j\pi((M_1-1)u_1+(N_1-1)v_1)}\\e^{-j\pi((M_1-1)u_2+(N_1-1)v_2)}\\\vdots\\e^{-j\pi((M_1-1)u_{K+1}+(N_1-1)v_{K+1})}\end{bmatrix}\right\} \tag{39}$$

accounts for the relationship $\mathbf{J}_{M_1N_1}\overline{\mathbf{D}}^*=\overline{\mathbf{D}}\mathbf{\Psi}$ according to (32). We observe from (36) that the effective source-correlation matrix on the SS subarray is given by

$$\overline{\mathbf{P}}=\frac{1}{2L}\sum_{i=1}^{M-M_1}\sum_{k=1}^{N-N_1}(\mathbf{\Phi}_{ik}\mathbf{G}\mathbf{P}\mathbf{G}^*\mathbf{\Phi}_{ik}^*+\mathbf{\Psi}\mathbf{\Phi}_{ik}^*\mathbf{G}^*\mathbf{P}^*\mathbf{G}\mathbf{\Phi}_{ik}\mathbf{\Psi}^*). \tag{40}$$

Discussions on the performance of 2-D spatial smoothing can be found in the literature.[10]

IV. SUBARRAY BEAMFORMER AND APERTURE RECOVERY

With the signal condition largely improved, the beamformer constructed on the SS subarray (master beamformer) should exhibit good SINR performance when applied back to an $M_1\times N_1$ regular subarray (slave beamformer). This section discusses the issues about the subarray beamformer and shows how a secondary combining recovers the full aperture of the original array.

A. Subarray beamformer

Denote as $\mathbf{W}_1$ the weight matrix acting on the SS subarray, and $\mathbf{w}_1=\mathrm{Vec}\{\mathbf{W}_1\}$ the corresponding vector representation. With the SS subarray-correlation matrix given by (33), the subarray beamformer can be obtained via the LCMV criterion similar to that described in Sec. I C, except that the following substitutions are made:

$$\mathbf{a}(u_o,v_o)\rightarrow\overline{\mathbf{a}}(u_o,v_o)$$

$$\mathbf{R}_x\rightarrow\overline{\mathbf{R}}_x^w=\overline{\mathbf{R}}_x-\overline{\sigma}_n^2\overline{\mathbf{R}}_n+\overline{\sigma}_n^2\mathbf{I}_{M_1N_1}, \tag{41}$$

which account for the change of array size and data-correlation structure. The second substitution involves a ''whitening'' process which replaces the noise part in $\overline{\mathbf{R}}_x$ by $\overline{\sigma}_n^2\mathbf{I}_{M_1N_1}$, where $\overline{\sigma}_n^2$ is an estimate of the noise power.[13] This is necessary since the subarray beamformer is to be applied on a regular subarray and should optimize itself with respect to the corresponding noise-correlation structure, which is $\sigma_n^2\mathbf{I}_{M_1N_1}$. With the substitutions of (41) in (12), we obtain the LCMV subarray weight vector:

$$\mathbf{w}_1=\frac{\sigma_n^2}{\sqrt{M_1N_1}}(\overline{\mathbf{R}}_x^w)^{-1}\overline{\mathbf{a}}(u_o,v_o), \tag{42}$$

and the corresponding weight matrix $\mathbf{W}_1=\mathrm{Vec}^{-1}\{\mathbf{w}_1\}$.

B. Aperture recovery via secondary combining

The subarray weight matrix $\mathbf{W}_1$ can be applied on any of the M_2N_2 subarrays of size $M_1\times N_1$, where $M_2=(M-M_1+1)$ and $N_2=(N-N_1+1)$. As long as a sufficient degree of freedom is maintained, the resulting subarray beamformer will produce a null in each of the K interfering directions. Unfortunately, working with a single subarray beamformer results in an aperture loss. A remedy would be to construct a beamformer for each subarray using the same weight matrix $\mathbf{W}_1$, and then linearly combine these beamformers using an $M_2\times N_2$ weight matrix $\mathbf{W}_2$. With this operation, $\mathbf{W}_2$ is regarded as the weight matrix acting on an $M_2\times N_2$ virtual subarray, on which each element (subarray beamformer) eliminates all the interferers in the same way due to the response pattern $w_1(u,v)=\mathbf{w}_1^H\overline{\mathbf{a}}(u,v)$. We refer to this virtual subarray as the ''interference cancellation'' (IC) subarray. The set of linearly combined subarray beamformers, as a whole, is effectively a full-aperture beamformer. This is illustrated in Fig. 3.

Denote as

$$\hat{\mathbf{A}}(u,v)=\mathbf{a}_{M_2}(u)\mathbf{a}_{N_2}^T(v) \tag{43}$$

$$\hat{\mathbf{a}}(u,v)=\mathrm{Vec}\{\hat{\mathbf{A}}(u,v)\} \tag{44}$$

the counterparts of $\mathbf{A}(u,v)$ and $\mathbf{a}(u,v)$, respectively associated with the IC subarray. Similar to (18)–(22), we can show that the IC subarray-data matrix is given by

$$\hat{\mathbf{X}}=\sum_{i=1}^{M_1}\sum_{k=1}^{N_1}\mathbf{W}_1^*(i,k)\mathbf{X}(i:i+M_2-1,k:k+N_2-1), \tag{45}$$

and the corresponding vector representation, which is more useful, can be obtained as

$$\begin{aligned}\hat{\mathbf{x}}&=\mathrm{Vec}\{\hat{\mathbf{X}}\}\\&=\mathbf{U}^H\mathbf{x}\approx\xi_1\mathbf{U}^H\mathbf{a}(u_1,v_1)+\mathbf{U}^H\mathbf{n}\\&=w_1(u_1,v_1)\xi_1\hat{\mathbf{a}}(u_1,v_1)+\mathbf{U}^H\mathbf{n},\end{aligned} \tag{46}$$

where

$$\mathbf{U}=\begin{bmatrix}\mathbf{U}_1 & & 0\\ \vdots & \mathbf{U}_1 & \\ \mathbf{U}_{N_1} & \vdots & \ddots\\ & \mathbf{U}_{N_1} & & \mathbf{U}_1\\ & & \ddots & \vdots\\ 0 & & & \mathbf{U}_{N_1}\end{bmatrix}_{MN\times M_2N_2} \tag{47}$$

with

$$\mathbf{U}_i=\begin{bmatrix}\mathbf{W}_1(1,i) & & & 0\\ \vdots & \mathbf{W}_1(1,i) & & \\ \mathbf{W}_1(M_1,i) & \vdots & \ddots & \\ & \mathbf{W}_1(M_1,i) & & \mathbf{W}_1(1,i)\\ & & \ddots & \vdots\\ 0 & & & \mathbf{W}_1(M_1,i)\end{bmatrix}_{M\times M_2}$$

$$i=1,\ldots,N_1 \tag{48}$$

is a Toeplitz–block–Toeplitz matrix representation of $\mathbf{W}_1$. Note that the approximation in (46) holds since the interference has been removed in the first-stage beamformer, and the last equality results due to $\mathbf{U}^H\mathbf{a}(u,v)=w_1(u_1,v_1)\hat{\mathbf{a}}(u,v)$.

Let $\mathbf{w}_2=\mathrm{Vec}\{\mathbf{W}_2\}$ be the vector representation of $\mathbf{W}_2$. The expression in (46) suggests that the combiner acting on the IC subarray should be chosen so as to maximize the output SNR in the look direction (u_o,v_o). That is,

$$\begin{aligned}&\max_{\mathbf{w}_2}\frac{E\{|w_1(u_1,v_1)\xi_1\mathbf{w}_2^H\hat{\mathbf{a}}(u_o,v_o)|^2\}}{E\{|\mathbf{w}_2^H\mathbf{U}^H\mathbf{n}|^2\}}\\&\quad\equiv\frac{|w_1(u_1,v_1)|^2\sigma_1^2}{\sigma_n^2}\frac{|\mathbf{w}_2^H\hat{\mathbf{a}}(u_o,v_o)|^2}{\mathbf{w}_2^H\mathbf{U}^H\mathbf{U}\mathbf{w}_2},\end{aligned} \tag{49}$$

which is equivalent to

$$\min_{\mathbf{w}_2}\mathbf{w}_2^H\mathbf{U}^H\mathbf{U}\mathbf{w}_2\quad\text{subject to:}\quad\mathbf{w}_2^H\hat{\mathbf{a}}(u_o,v_o)=c. \tag{50}$$

This is again an LCMV-type problem whose solution is given by

$$\mathbf{w}_2=\frac{\sigma_n^2}{\sqrt{M_2N_2}}(\mathbf{U}^H\mathbf{U})^{-1}\hat{\mathbf{a}}(u_o,v_o). \tag{51}$$

Finally, the weight matrix is recovered via $\mathbf{W}_2=\mathrm{Vec}^{-1}\{\mathbf{w}_2\}$.

C. Structure and behavior of the full-aperture beamformer

The full-aperture weight matrix is obtained by the 2-D convolution of the two-stage subarray weight matrices $\mathbf{W}_1$ and $\mathbf{W}_2$:

$$\mathbf{W}(i,k)=\sum_{l=1}^{M_1}\sum_{m=1}^{N_1}\mathbf{W}_1(l,m)\mathbf{W}_2(i-l+1,k-m+1) \tag{52}$$

for $i=1,...,M$, $k=1,...,N$. The vector representation of $\mathbf{W}$ can be derived from (52), or by comparing (9) with $y=\mathbf{w}_2^H\hat{\mathbf{x}}=\mathbf{w}_2^H\mathbf{U}^H\mathbf{x}$ as observed in (46):

$$\mathbf{w}=\mathbf{U}\mathbf{w}_2=\mathbf{U}(\mathbf{U}^H\mathbf{U})^{-1}\hat{\mathbf{a}}(u_o,v_o)\propto\mathbf{U}(\mathbf{U}^H\mathbf{U})^{-1}\mathbf{U}^H\mathbf{a}(u_o,v_o). \tag{53}$$

It is interesting to note that the last expression in (53) can be interpreted algebraically as the orthogonal projection of $\mathbf{a}(u_o,v_o)$ onto the range space of $\mathbf{U}$. This makes sense, since $\mathbf{a}(u_o,v_o)$ is the optimum weight vector which maximizes the beamformer output SNR under the quiescent (spatially white-noise-only) condition. On the other hand, the range space of $\mathbf{U}$ represents the ''subspace of interference cancellation.'' Projecting $\mathbf{a}(u_o,v_o)$ onto the range space of $\mathbf{U}$ is equivalent to finding a vector lying in the subspace of interference cancellation which is closest to the optimum quiescent weight vector.

By applying the full-aperture weight vector $\mathbf{w}$ to the original array, a beamformer results which suppresses the interferers individually and nearly achieves the maximum SNR gain of the quiescent beamformer. Nevertheless, it should be pointed out that although the secondary combining can enhance the performance of the beamformer against uncorrelated noise, it cannot restore the interference cancellation capability of the original array. This is because interference cancellation is done entirely on the first-stage beamformer, and thus limited in performance by the subarray size. For example, interferers that are close to each other, or close to the look direction, will not be canceled successfully by the full-aperture beamformer due to the reduced resolution of the subarray. Some prior information about the interference scenario can help to determine a suitable subarray size to avoid this reduced aperture effect.

V. PERFORMANCE ANALYSIS OF THE TWO-STAGE BEAMFORMER

The following sections derive the output SINR of the two-stage beamformer for some cases of interest. The derivations are all based on the true ensemble data-correlation matrix. For a manageable analysis, we consider the case of two interferers ($K=2$) and make the following assumptions:

A1. No interfering signals are eliminated by the difference preprocessor.
A2. The interfering signals are nearly uncorrelated on the SS subarray.
A3. The desired signal is negligible compared to the interfering signals and noise on the SS subarray.
A4. The interference directions are well away from the look direction.

For brevity, some shorthand notations are defined as follows:

$$\overline{\mathbf{a}}_i=\overline{\mathbf{a}}(u_i,v_i)\quad i=o,1,2,3$$

$$\hat{\mathbf{a}}_i=\hat{\mathbf{a}}(u_i,v_i)\quad i=o,1,2,3$$

$$\kappa_i=|h(u_i,v_i)|^2\quad i=2,3$$

$$\gamma_i=\frac{\sigma_i^2}{\sigma_n^2}\quad i=1,2,3,$$

where we note that γ_1 denotes the input SNR, and γ_2 and γ_3 denote the input INR.

A. Output SINR of the first-stage beamformer

Under A1–A3, we can express the whitened SS subarray-correlation matrix in the following form:

$$\overline{\mathbf{R}}_x^w\approx\kappa_2\sigma_2^2\overline{\mathbf{a}}_2\overline{\mathbf{a}}_2^H+\kappa_3\sigma_3^2\overline{\mathbf{a}}_3\overline{\mathbf{a}}_3^H+\sigma_n^2\mathbf{I}_{M_1N_1}. \tag{54}$$

Using the matrix inversion lemma, we get

$$(\overline{\mathbf{R}}_x^w)^{-1}=\sigma_n^{-2}\left\{\mathbf{I}_{M_1N_1}-[\kappa_2\gamma_2\overline{\mathbf{a}}_2\quad\kappa_3\gamma_3\overline{\mathbf{a}}_3]\mathbf{\Gamma}^{-1}\begin{bmatrix}\overline{\mathbf{a}}_2^H\\ \overline{\mathbf{a}}_3^H\end{bmatrix}\right\}, \tag{55}$$

where

$$\mathbf{\Gamma}=\begin{bmatrix}1+M_1N_1\kappa_2\gamma_2 & M_1N_1\kappa_3\gamma_3\overline{\rho}_{23}\\ M_1N_1\kappa_2\gamma_2\overline{\rho}_{32} & 1+M_1N_1\kappa_3\gamma_3\end{bmatrix} \tag{56}$$

with

$$\overline{\rho}_{ik}=\frac{\overline{\mathbf{a}}_i^H\overline{\mathbf{a}}_k}{M_1N_1}=\frac{\sin\left(\frac{\pi}{2}M_1(u_k-u_i)\right)\sin\left(\frac{\pi}{2}N_1(v_k-v_i)\right)}{\sin\left(\frac{\pi}{2}(u_k-u_i)\right)\sin\left(\frac{\pi}{2}(v_k-v_i)\right)}\times e^{j(\pi/2)((M_1-1)(u_k-u_i)+(N_1-1)(v_k-v_i))}$$

$$i,k=o,1,2,3 \tag{57}$$

being the cosine angles between $\overline{\mathbf{a}}_i$ and $\overline{\mathbf{a}}_k$. Substituting (55) into (42) yields the first-stage weight vector:

$$\mathbf{w}_1=\frac{1}{\sqrt{M_1N_1}}\left\{\overline{\mathbf{a}}_o-[\kappa_2\gamma_2\overline{\mathbf{a}}_2\quad\kappa_3\gamma_3\overline{\mathbf{a}}_3]\mathbf{\Gamma}^{-1}\begin{bmatrix}M_1N_1\overline{\rho}_{2o}\\ M_1N_1\overline{\rho}_{3o}\end{bmatrix}\right\}$$

$$=\frac{1}{\sqrt{M_1N_1}}(\overline{\mathbf{a}}_o-\alpha\overline{\mathbf{a}}_2-\beta\overline{\mathbf{a}}_3), \tag{58}$$

where

$$\alpha=\frac{M_1N_1\kappa_2\gamma_2[\overline{\rho}_{2o}+M_1N_1\kappa_3\gamma_3(\overline{\rho}_{2o}-\overline{\rho}_{23}\overline{\rho}_{3o})]}{1+M_1N_1(\kappa_2\gamma_2+\kappa_3\gamma_3)+M_1^2N_1^2\kappa_2\kappa_3\gamma_2\gamma_3(1-|\overline{\rho}_{32}|^2)}, \tag{59}$$

$$\beta=\frac{M_1N_1\kappa_3\gamma_3[\overline{\rho}_{3o}+M_1N_1\kappa_2\gamma_2(\overline{\rho}_{3o}-\overline{\rho}_{32}\overline{\rho}_{2o})]}{1+M_1N_1(\kappa_2\gamma_2+\kappa_3\gamma_3)+M_1^2N_1^2\kappa_2\gamma_2\kappa_3\gamma_3(1-|\overline{\rho}_{32}|^2)}. \tag{60}$$

Denote as P_s, P_I, and P_n the desired signal, interference, and noise beamformer output powers, respectively. By A1–A4, $\mathbf{w}_1$ suppresses each of the interferers such that P_I is negligible compared to P_s and P_n. As a result, the output SINR of the first-stage beamformer is given approximately by

$$\mathrm{SINR}_1=\frac{P_s}{P_I+P_n}\approx\frac{P_s}{P_n}=\frac{|\mathbf{w}_1^H\overline{\mathbf{a}}_1|^2}{\mathbf{w}_1^H\mathbf{w}_1}\,\gamma_1. \tag{61}$$

Substitution of (58) into the above gives

$$\mathrm{SINR}_1 \approx \frac{|(\bar{\mathbf{a}}_o - \alpha\bar{\mathbf{a}}_2 - \beta\bar{\mathbf{a}}_3)^H \bar{\mathbf{a}}_1|^2}{(\bar{\mathbf{a}}_o - \alpha\bar{\mathbf{a}}_2 - \beta\bar{\mathbf{a}}_3)^H(\bar{\mathbf{a}}_o - \alpha\bar{\mathbf{a}}_2 - \beta\bar{\mathbf{a}}_3)}$$
$$= \frac{M_1 N_1 |\bar{\rho}_{o1} - \alpha^*\bar{\rho}_{21} - \beta^*\bar{\rho}_{31}|^2 \gamma_1}{1 + |\alpha|^2 + |\beta|^2 - 2\,\mathrm{Re}\{\alpha^*\bar{\rho}_{2o} + \beta^*\bar{\rho}_{3o} - \alpha\beta^*\bar{\rho}_{32}\}} \times \gamma_1 . \tag{62}$$

Some cases of interest are considered below.

1. Case 1: High-input INR

With the assumption of high-input INR ($\gamma_i \gg 1$, $i=2,3$) and that κ_2 and κ_3 are not too small, we have

$$\alpha \approx \frac{\bar{\rho}_{2o} - \bar{\rho}_{23}\bar{\rho}_{3o}}{1 - |\bar{\rho}_{32}|^2}, \tag{63}$$

$$\beta \approx \frac{\bar{\rho}_{3o} - \bar{\rho}_{32}\bar{\rho}_{2o}}{1 - |\bar{\rho}_{32}|^2}. \tag{64}$$

Substituting these into (62), along with some algebraic manipulations, we get

$$\mathrm{SINR}_1 \approx \frac{M_1 N_1 |\bar{\rho}_{o1}(1 - |\bar{\rho}_{32}|^2) - \bar{\rho}_{21}\bar{\rho}_{o2} - \bar{\rho}_{31}\bar{\rho}_{o3} + \bar{\rho}_{o3}\bar{\rho}_{32}\bar{\rho}_{21} + \bar{\rho}_{o2}\bar{\rho}_{23}\bar{\rho}_{31}|^2}{(1 - |\bar{\rho}_{32}|^2)(1 + 2\bar{\rho}_{32}\bar{\rho}_{2o}\bar{\rho}_{o3} - |\bar{\rho}_{2o}|^2 - |\bar{\rho}_{3o}|^2 - |\bar{\rho}_{32}|^2)}\ \gamma_1 . \tag{65}$$

In particular, with a small pointing error ($u_o \approx u_1$, $v_o \approx v_1$), we have $\bar{\rho}_{1o} \approx 1$ and $\bar{\rho}_{oi} \approx \bar{\rho}_{1i}$, $i=2,3$, such that (65) reduces to

$$\mathrm{SINR}_1 \approx M_1 N_1 \left(1 - \frac{|\bar{\rho}_{21}|^2 + |\bar{\rho}_{31}|^2 - 2\bar{\rho}_{21}\bar{\rho}_{13}\bar{\rho}_{32}}{1 - |\bar{\rho}_{32}|^2}\right)\gamma_1 . \tag{66}$$

2. Case 2: Low-input INR or orthogonal interference directions

With a low-input INR ($\gamma_i \approx 0$, $i=2,3$) and/or orthogonal interference directions ($\bar{\rho}_{io} \approx 0$, $i=2,3$), we have $\alpha \approx 0$ and $\beta \approx 0$ such that

$$\mathbf{w}_1 \approx \frac{1}{\sqrt{M_1 N_1}}\,\bar{\mathbf{a}}_o , \tag{67}$$

and (62) reduces to

$$\mathrm{SINR}_1 \approx M_1 N_1 |\bar{\rho}_{o1}|^2 \gamma_1 , \tag{68}$$

which is the result obtained under the quiescent condition. Finally, with a small pointing error, we get

$$\mathrm{SINR}_1 \approx M_1 N_1 \gamma_1 , \tag{69}$$

which is simply the maximum-output SNR of the optimum quiescent beamformer.[6]

B. Output SINR of the overall beamformer

Using (46) and (51), the output SINR of the overall two-stage beamformer (as observed at the second-stage beamformer output) is given by

$$\mathrm{SINR}_o \approx \frac{|\mathbf{w}_2^H \hat{\mathbf{a}}_1|^2}{\mathbf{w}_2^H \mathbf{U}^H \mathbf{U} \mathbf{w}_2}\,|w_1(u_1, v_1)|^2 \gamma_1$$
$$= \hat{\mathbf{a}}_1^H (\mathbf{U}^H \mathbf{U})^{-1} \hat{\mathbf{a}}_1 |\hat{\rho}_{1o}|^2 |w_1(u_1, v_1)|^2 \gamma_1 , \tag{70}$$

where

$$\hat{\rho}_{1o} = \frac{\hat{\mathbf{a}}_1^H (\mathbf{U}^H \mathbf{U})^{-1} \hat{\mathbf{a}}_o}{[\hat{\mathbf{a}}_o^H (\mathbf{U}^H \mathbf{U})^{-1} \hat{\mathbf{a}}_o \hat{\mathbf{a}}_1^H (\mathbf{U}^H \mathbf{U})^{-1} \hat{\mathbf{a}}_1]^{1/2}}. \tag{71}$$

Again, two cases are considered below.

1. Case 1: High-input INR

With a high-input INR, we have from (58), (63), and (64)

$$w_1(u_1, v_1) \approx \sqrt{M_1 N_1}\left(\bar{\rho}_{o1} - \frac{\bar{\rho}_{21}\bar{\rho}_{o2} + \bar{\rho}_{31}\bar{\rho}_{o3} - \bar{\rho}_{o3}\bar{\rho}_{32}\bar{\rho}_{21} - \bar{\rho}_{o2}\bar{\rho}_{23}\bar{\rho}_{31}}{1 - |\bar{\rho}_{32}|^2}\right). \tag{72}$$

Substituting this into (70) yields

$$\mathrm{SINR}_o \approx \hat{\mathbf{a}}_1^H (\mathbf{U}^H \mathbf{U})^{-1} \hat{\mathbf{a}}_1 |\hat{\rho}_{1o}|^2 M_1 N_1 \left|\bar{\rho}_{o1} - \frac{\bar{\rho}_{21}\bar{\rho}_{2o} + \bar{\rho}_{31}\bar{\rho}_{3o} - \bar{\rho}_{21}\bar{\rho}_{o3}\bar{\rho}_{32} - \bar{\rho}_{31}\bar{\rho}_{o2}\bar{\rho}_{23}}{1 - |\bar{\rho}_{32}|^2}\right|^2 \gamma_1 . \tag{73}$$

With a small pointing error, we have $\hat{\rho}_{1o} \approx 1$ such that

$$\mathrm{SINR}_o \approx \hat{\mathbf{a}}_1^H (\mathbf{U}^H \mathbf{U})^{-1} \hat{\mathbf{a}}_1 M_1 N_1 \times \left(1 - \frac{|\bar{\rho}_{21}|^2 + |\bar{\rho}_{31}|^2 - 2\bar{\rho}_{21}\bar{\rho}_{13}\bar{\rho}_{32}}{1 - |\bar{\rho}_{32}|^2}\right)^2 \gamma_1$$
$$= \hat{\mathbf{a}}_1^H (\mathbf{U}^H \mathbf{U})^{-1} \hat{\mathbf{a}}_1 \left(1 - \frac{|\bar{\rho}_{21}|^2 + |\bar{\rho}_{31}|^2 - 2\bar{\rho}_{21}\bar{\rho}_{13}\bar{\rho}_{32}}{1 - |\bar{\rho}_{32}|^2}\right) \times \mathrm{SINR}_1 , \tag{74}$$

where we have used (66).

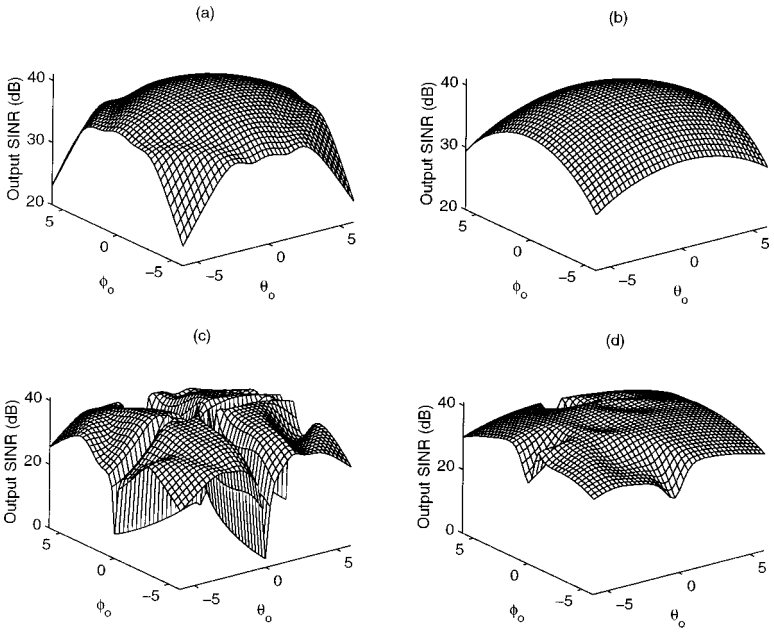

FIG. 4. Output SINR versus pointing error. $M_1=5$, $N_1=6$. $(\theta_1,\phi_1)=(0\ \text{deg},0\ \text{deg})$. $\mu=1$. (a) separable preprocessor. $(\theta_2,\phi_2)=(20\ \text{deg},20\ \text{deg})$, $(\theta_3,\phi_3)=(40\ \text{deg},40\ \text{deg})$. (b) nonseparable preprocessor. $(\theta_2,\phi_2)=(20\ \text{deg},20\ \text{deg})$, $(\theta_3,\phi_3)=(40\ \text{deg},40\ \text{deg})$. (c) separable preprocessor. $(\theta_2,\phi_2)=(0\ \text{deg},20\ \text{deg})$, $(\theta_3,\phi_3)=(40\ \text{deg},0\ \text{deg})$. (d) nonseparable preprocessor. $(\theta_2,\phi_2)=(0\ \text{deg},20\ \text{deg})$, $(\theta_3,\phi_3)=(40\ \text{deg},0\ \text{deg})$.

2. Case 2: Low-input INR or orthogonal interference directions

With a low-input INR and/or orthogonal interference directions, we have from the previous results that $w_1(u_1,v_1)=\sqrt{M_1N_1\overline{\rho}_{o1}}$ such that

$$\begin{aligned}\text{SINR}_o &\approx \hat{\mathbf{a}}_1(\mathbf{U}^H\mathbf{U})^{-1}\hat{\mathbf{a}}_1|\hat{\rho}_{1o}|^2M_1N_1|\overline{\rho}_{o1}|^2\gamma_1\\ &=\hat{\mathbf{a}}_1(\mathbf{U}^H\mathbf{U})^{-1}\hat{\mathbf{a}}_1|\hat{\rho}_{1o}|^2\text{SINR}_1,\end{aligned}\tag{75}$$

which means that the second-stage beamformer exhibits an SNR gain of $\hat{\mathbf{a}}_1^H(\mathbf{U}^H\mathbf{U})^{-1}\hat{\mathbf{a}}_1|\hat{\rho}_{1o}|^2$. Finally, the optimum quiescent beamformer output SINR is achieved with a small pointing error:

$$\text{SINR}_o\approx\hat{\mathbf{a}}_1^H(\mathbf{U}^H\mathbf{U})^{-1}\hat{\mathbf{a}}_1M_1N_1\gamma_1.\tag{76}$$

Although no closed-form expression of (76) is given, we have found by simulation that the maximum two-stage output SINR is fairly close to $MN\gamma_1$, which is the optimum one-stage output SINR achieved by the quiescent beamformer.

VI. SIMULATION RESULTS

Computer simulations on narrow-band signal extraction were conducted to ascertain the performance of the two-stage beamformer. The array was 10×12 with identical sensors equally spaced by a half-wavelength of the sources. The desired signal arrived from $(\theta_1,\phi_1)=(0\ \text{deg},0\ \text{deg})$, with an SNR of 20 dB. Except for one case, we put two interferers at $(\theta_2,\phi_2)=(20\ \text{deg},20\ \text{deg})$ and $(\theta_3,\phi_3)=(40\ \text{deg},40\ \text{deg})$, respectively, with the same INR of 30 dB. The source-correlation matrix, as defined in Sec. I C, was set to be

$$\mathbf{P}=\begin{bmatrix}\sigma_1^2 & \mu^*\sigma_1\sigma_2 & \mu^*\sigma_1\sigma_3\\ \mu\sigma_2\sigma_1 & \sigma_2^2 & \mu^*\sigma_2\sigma_3\\ \mu\sigma_3\sigma_1 & \mu\sigma_3\sigma_2 & \sigma_3^2\end{bmatrix},$$

which says that the three sources are mutually correlated with the same correlation coefficient μ. To measure the interference suppression performance of the two-stage beamformer, we defined the simulated output SINR as

$$\text{SINR}_o=\frac{\sigma_1^2\mathbf{w}^H\mathbf{a}_1\mathbf{a}_1^H\mathbf{w}}{\sigma_n^2\mathbf{w}^H\mathbf{w}+\Sigma_{i=2}^3\Sigma_{k=2}^3\mathbf{P}(i,k)\mathbf{w}^H\mathbf{a}_i\mathbf{a}_k^H\mathbf{w}}.$$

In all cases, we assumed that the three sources and noise were stationary over the processing period of the beamformer, and a sufficient amount of data were available such that the ensemble-correlation matrix and weight vectors could be obtained.

The first set of simulations examines the SINR performance of the two-stage beamformer against pointing errors. The look direction (θ_o,ϕ_o) was varied over the angular region $\{-6\ \text{deg}\leqslant\theta_o\leqslant6\ \text{deg},\ -6\ \text{deg}\leqslant\phi_o\leqslant6\ \text{deg}\}$. A coherent scenario was assumed by setting $\mu=1$. The subarray size was chosen as $M_1=5$, $N_1=6$. The resulting output SINR plots obtained with the separable and nonseparable (with $\epsilon=10^{-4}$) difference preprocessors are shown in Fig. 4(a) and (b), respectively. As expected, the output SINR drops as the pointing error increases. This is more significant for the separable preprocessor with a large pointing error. To see the result when the interferers are inside the cross-null region of $h(u,v)$, we changed the interference directions to $(\theta_2,\phi_2)=(0\ \text{deg},20\ \text{deg})$ and $(\theta_3,\phi_3)=(40\ \text{deg},0\ \text{deg})$, and repeated the above simulations. The results shown in Fig. 4(c) and (d) indicate that the separable preprocessor breaks down when θ_o or ϕ_o is zero. This is the case where at least one of the interferers is eliminated by $h(u,v)$. On the other hand, the nonseparable preprocessor performed reliably for a small pointing error, though certain degradation occurred near the four edges. In the remaining examples, only the nonseparable preprocessor (with $\epsilon=10^{-4}$) will be used.

The second set of simulations investigates the effect of subarray size. In this case, M_1 was varied from 2 to 9, and N_1 from 2 to 11. Fig. 5(a) and (b) show the output SINR plots obtained with $(\theta_o,\phi_o)=(0\ \text{deg},0\ \text{deg})$ and $(\theta_o,\phi_o)=(3\ \text{deg},3\ \text{deg})$, respectively, for $\mu=1$. Figure 5(c) and (d) show the corresponding results for $\mu=j$. We observe that

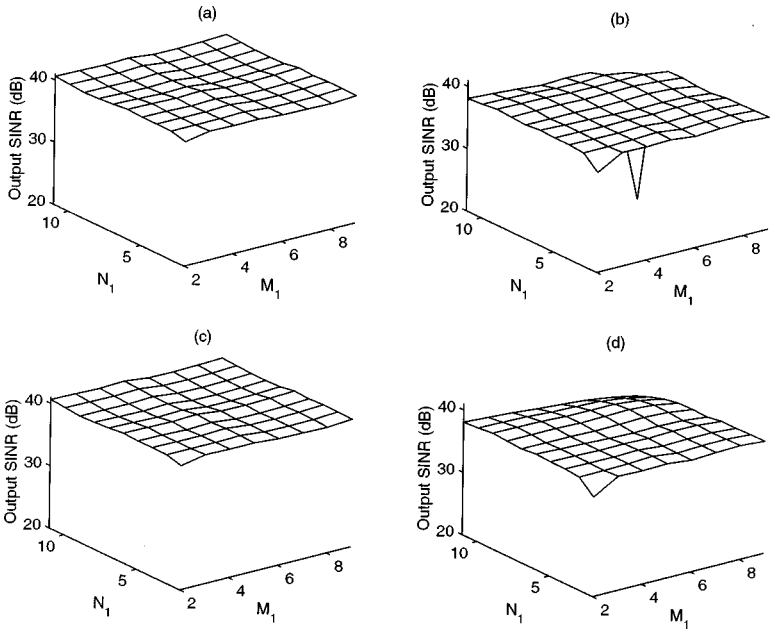

FIG. 5. Output SINR versus subarray size. $(\theta_1,\phi_1)=(0\ \text{deg},0\ \text{deg})$, $(\theta_2,\phi_2)=(20\ \text{deg},20\ \text{deg})$, $(\theta_3,\phi_3)=(40\ \text{deg},40\ \text{deg})$. (a) $(\theta_0,\phi_0)=(0\ \text{deg},0\ \text{deg})$. $\mu=1$. (b) $(\theta_0,\phi_0)=(3\ \text{deg},3\ \text{deg})$. $\mu=1$. (c) $(\theta_0,\phi_0)=(0\ \text{deg},0\ \text{deg})$. $\mu=j$. (d) $(\theta_0,\phi_0)=(3\ \text{deg},3\ \text{deg})$. $\mu=j$.

the output SINR is insensitive to the subarray size so long as a sufficient degree of freedom is given for interference cancellation. This also demonstrates that aperture recovery can be done successfully for any suitably chosen subarray size. In particular, the SINR achieved without pointing error is close to the optimum value $(10\log_{10}120+20=40.8)$ for all possible subarray sizes, except for the extreme cases of $M_1=N_1=2$, and $M_1=9$, $N_1=11$. Note that the performance breakdown with $M_1=9$, $N_1=11$ and $\mu=1$ in the presence of pointing errors was due to the mutual cancellation between the desired signal and interference as a result of poor decorrelation. This did not happen with $\mu=j$, for which effective decorrelation was achieved with FB averaging.

In the third set of simulations, we evaluate the effect of the correlation coefficient. The amplitude $(|\mu|)$ and phase $[\text{angle}(\mu)]$ of μ were varied from 0 to 1 and 0 to π, respectively. Figure 6(a) and (b) show the output SINR obtained with $(\theta_o,\phi_o)=(0\ \text{deg},0\ \text{deg})$ and $(\theta_o,\phi_o)=(3\ \text{deg},3\ \text{deg})$, respectively, for $M_1=5$, $N_1=6$. The results show that the proposed beamformer is robust to the change of μ. The simulation was then repeated with $M_1=9$, $N_1=11$ (no smoothing) and the results were plotted in Fig. 6(c) and (d). Surprisingly, the output SINR without pointing error did not exhibit any degradation. This is because the mutual cancellation between the two interferers was not significantly affected by the difference preprocessor. On the other hand, the beamformer suffered performance breakdown with pointing errors for $\mu\approx\pm1$, which is the case where FB averaging has almost no effect. This again ascertains that the proposed beamformer performs reliably with a properly chosen subarray size.

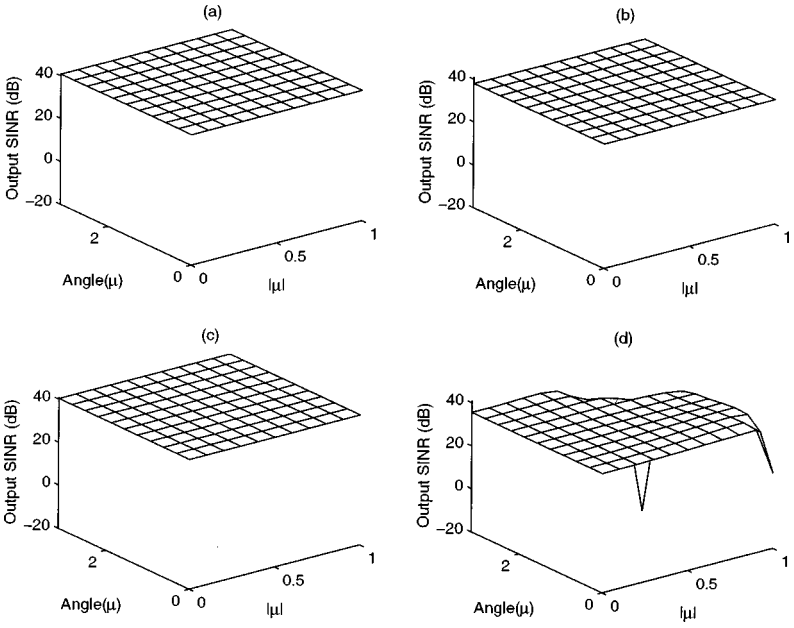

FIG. 6. Output SINR versus correlation coefficient. $(\theta_1,\phi_1)=(0\ \text{deg},0\ \text{deg})$, $(\theta_2,\phi_2)=(20\ \text{deg},20\ \text{deg})$. $(\theta_3,\phi_3)=(40\ \text{deg},40\ \text{deg})$. (a) $(\theta_0,\phi_0)=(0\ \text{deg},0\ \text{deg})$. $M_1=5$, $N_1=6$. (b) $(\theta_0,\phi_0)=(3\ \text{deg},3\ \text{deg})$. $M_1=5$, $N_1=6$. (c) $(\theta_0,\phi_0)=(0\ \text{deg},0\ \text{deg})$. $M_1=9$, $N_1=11$. (d) $(\theta_0,\phi_0)=(3\ \text{deg},3\ \text{deg})$. $M_1=9$, $N_1=11$.

VII. CONCLUSION

We have presented a two-stage 2-D adaptive beamforming scheme for combating multiple correlated interferers using a rectangular array. By difference preprocessing and spatial smoothing, a virtual subarray was obtained on which the desired-signal strength and correlation among interferers were reduced to a negligible order. An LCMV-type beamformer constructed on this smoothed subarray is ideal for desired-signal acquisition, but inefficient in terms of aperture utilization. A post-beamformer based on the maximum SNR criterion was thus employed in the second stage to recover the full array aperture. The derivation of the weight vector was eased by exploiting the distinctive Toeplitz–block–Toeplitz structure due to 2-D convolution. For a theoretical performance evaluation, an analysis on the output SINR of the proposed beamformer was presented for some cases of interest. Finally, the behavior of the proposed beamformer was examined and discussed via several sets of computer simulations. In particular, it was shown that the performance of the two-stage beamformer is fairly reliable approaching that of the optimum one-stage beamformer, provided that a suitable subarray size is chosen for successfully decorrelating the interference. The proposed beamformer is suitable for acoustical applications such as remote sound-source enhancement in a large room or subsea acoustical communications operated in shallow water, for which correlated multipaths cause a major problem.

ACKNOWLEDGMENT

This work was supported by the National Science Council of R.O.C. under Grant NSC 84-2213-E-009-119.

[1] R. A. Monzingo and T. W. Miller, *Introduction to Adaptive Arrays* (Wiley, New York, 1980).

[2] J. L. Flanagan, J. D. Johnston, R. Zahn, and G. W. Elko, ''Computer-steered microphone arrays for sound transduction in large rooms,'' J. Acoust. Soc. Am. **78**, 1508–1518 (1985).

[3] I. Claesson, S. E. Nordholm, B. A. Bengtsson, and P. Eriksson, ''A multi-DSP Implementation of a broad-band adaptive beamformer for use in a hands-free mobile radio telephone,'' IEEE Trans. Veh. Technol. **VT-40**, 194–202 (1991).

[4] G. S. Howe, P. S. D. Tarbit, O. R. Hinton, B. S. Sharif, and A. E. Adams, ''Subsea remote communications utilising an adaptive receiving beamformer for multipath suppression,'' Proc. IEEE Oceans Conf. **1**, 313–316 (1994).

[5] B. Widrow, K. M. Duvall, R. P. Gooch, and W. C. Newman, ''Signal cancellation phenomena in adaptive antennas: causes and cures,'' IEEE Trans. Antennas Propag. **AP-30**, 469–478 (1982).

[6] L. C. Godara, ''Error analysis of the optimal antenna processors,'' IEEE Trans. Aerosp. Electron. Syst. **AES-22**, 395–400 (1986).

[7] A. K. Luthra, ''A solution to adaptive nulling problem with a look-direction constraint in the presence of coherent jammers,'' IEEE Trans. Antennas Propag. **AP-34**, 702–710 (1986).

[8] T. J. Shan and T. Kailath, ''Adaptive beamforming for coherent signals and interference,'' IEEE Trans. Acoust., Speech, Signal Process. **ASSP-33**, 527–536 (1985).

[9] T. S. Lee and T. K. Tseng, ''Subarray-synthesized low-side-lobe sum and difference patterns with partial common weights,'' IEEE Trans. Antennas Propag. **AP-41**, 791–800 (1993).

[10] Y. M. Chen, ''On spatial smoothing for two-dimensional direction-of-arrival estimation of coherent signals,'' IEEE Trans. Signal Process. **SP-45**, 1689–1696 (1997).

[11] B. D. Van Veen and K. M. Buckley, ''Beamforming: A versatile approach to spatial filtering,'' IEEE ASSP Mag. **5**, 4–24 (1988).

[12] S. U. Pillai and B. H. Kwon, ''Forward/backward spatial smoothing techniques for coherent signal identification,'' IEEE Trans. Acoust., Speech, Signal Process. **ASSP-37**, 8–15 (1989).

[13] P. Stoica, T. Söderström and V. Šimonytė, ''On estimating the noise power in array processing,'' Signal Process. **26**, 205–220 (1992).